SCIENTIFIC REPORTS

OPEN

SUBJECT AREAS:
ELECTRONICS, PHOTONICS AND DEVICE PHYSICS
NANOSCALE DEVICES
ELECTROCHEMISTRY

Received
29 October 2013

Accepted
8 November 2013

Published
25 November 2013

Correspondence and requests for materials should be addressed to Y.-Y.S. (yysong@mail.neu.edu.cn)

One-Step to Prepare Self-Organized Nanoporous NiO/TiO_2 Layers and its Use in Non-Enzymatic Glucose Sensing

Zhi-Da Gao, Yuyao Han, Yongmei Wang, Jingwen Xu & Yan-Yan Song

College of Sciences, Northeastern University, Shenyang 110004, China.

A highly ordered nanoporous NiTi oxide layers were fabricated on Ti alloys with high Ni contents (50.6 at.%) by a combination of self-organizing anodization at 0°C and subsequent selective etching in H_2O_2. The key for successful formation of such layers is to sufficiently suppress the dissolve of NiO by applying lower temperature during anodization. The resulting nanoporous structure is connected and well-adhered, which exhibits a much higher electrochemical cycling stability in 0.1 M NaOH. Without further surface modification or the use of polymer binders, the layers can be behave as a low-cost, stable and sensitive platform in non-enzymatic glucose sensing.

Fast, sensitive and reliable glucose monitoring is important for clinical biochemistry and food industry[1,2]. Since Clark proposed the first enzyme glucose biosensor in 1962[3], it has attracted considerable attention. However, due to the use of enzymes, conventional glucose sensors usually suffer from short device lifetime and decay in activity, and their performances are easily affected by the variation in temperature and pH value during measurement. This limitation can be overcome by the use of non-enzymatic glucose sensors based on noble metal or metal oxides[4–8]. To achieve better device lifetime and stability in non-enzymatic sensing, basically a mixture of electrochemically active materials (such as Pt, Pd) and conducting binders (such as Nafion) is typically pasted onto a glassy carbon electrode to construct a stable network[9–11]. However, polymer binders are not active materials for glucose sensing, and lead to a blocking of electrocatalytic sites. Additionally, because of the increasing price of noble metals and easy poisoning of their surface, their application in glucose sensing is limited. The nickel (Ni)-based electrode has been the most widely utilized electrode for determining glucose in alkaline media[12,13], since Fleischmann demonstrated that glucose molecules could be oxidized at a nickel anode in alkaline solution[14]. Recently, some $NiO/Ni(OH)_2$ electrodes were prepared by depositing Ni particles on a traditional electrode surface (i.e. Au, glassy carbon)[15]. The resulted electrodes can improve the sensitivity and reproducibility for the determination of carbohydrates. However, a problem is that it is difficult to maintain long-term stability because of the detachment and dissolution of the catalyst from the substrate. Therefore, NiO nanoplatelets or nickel alloy-based electrodes were developed in order to improve the stability of the determination[16–18]. Kuwana *et al.* reported a systematic study of Ni-Cr and Ni-Ti alloy electrodes for the detection of carbohydrates[17,18]. Owing to the good resistance to surface fouling, these alloy electrodes exhibited improved long-term stability. However, the sensitivity of the alloy electrode is usually lower than the traditional nickel-modified electrodes. Xia and coworkers have revealed due to the increased surface area, the three-dimensional (3D) nanomaterials exhibited good electrochemical activity towards glucose non-enzymatic sensing[4–8].

Self-organizing electrochemical anodization is a simple, attractive and low-cost approach to form 3D nanostructures of metal oxides. In 1995, Masuda and Fukuda firstly fabricated highly ordered porous alumina structures by establishing optimized oxide formation/dissolution equilibrium during anodization of aluminium in an acidic solution[19]. Zwilling and coworkers demonstrated that self-organized TiO_2 nanopores or nanotubes can also be achieved through anodization of Ti foils in a fluoride-containing electrolyte in 1999[20]. Till now, the electrochemical annodization method has been applied to fabricate oxide nanotube or nanopore on numerous other metals such as V, Fe, W, Zr, Nb, V and Co, as well as many alloys[21–28].

Nevertheless, up to now, success on anodization of Ni-Ti alloy containing high content of nickel to obtain porous nanostructure is very challenging and such success has not been achieve yet because nickel hardly forms passive oxide layer on anodization and undergoes preferential electrochemical metal dissolution upon anodization. And the preferred reaction is the oxidation of the water at a comparably low potential when an anodic voltage is applied in an aqueous electrolyte. The evolution of oxygen will change pH of the neutral electrolyte to a

low value, which could leads to the dissolution of NiO in an acid aqueous electrolyte. Herein, we show how to overcome the problem by combining a number of strategies to retard the reaction rate of water oxidation and favor oxide formation. This enables the successful anodic growth of highly ordered nanoporous layers on a NiTi alloy. The resulting nanoporous oxide layers, after an appropriate treatment, not only show strongly enhanced sensitivity, but also provide wide linear range for the determination of glucose in comparison to chemically modified Nickel electrodes. Moreover, this approach, where an alloy is used to grow oxide tubes, is found to be much more efficient than other attempts to achieve a similar effect by decorating pure TiO_2 nanotubes with NiO nanoparticles.

Results

Fig. 1A–C show SEM top view of the samples formed on a NiTi foil after anodization at room temperature (RT), 10°C and 0°C for 8 h, respectively. And the corresponding current–time profiles are plotted in Fig. 1D. Obviously, in the case of NiTi anodization, the temperature influences the anodization currents and morphology of the nanostructures. A sufficiently steady-state current leading to self-organization is only achievable when the anodization is performed at sufficiently low temperature to slow down the anodization reaction and prevent current self-amplification because of resistive heating with continuously increasing currents and an ill-defined mix of O_2 evolution[27]. For the anodization performed at RT and 10°C, after some hours of anodization, dissolution (current increase) is observed and a large portion of the surface is found to peel off (inset SEM image of Fig. 1A) for prolonged anodization. Due to the dissolution of as formed NiO/TiO_2 layers, as shown in the digital photographs in insets of Fig. 1A and Fig. 1B, the sample surface is etched and the significant depressed areas can be noticed at RT and 10°C. The SEM images also exhibit the nanostructured layer formed at RT (Fig. 1A) and 10°C (Fig. 1B) is very thin. Even it's hard to scratch and measure the thickness of the oxide layers formed on the NiTi substrates. A very good indication for a successful growth of a well-defined nanoporous structure is the current curve which recorded at the 0°C. As shown in Fig. 1C, the as-formed nanostructure has a comparably tight oxide morphology with some nanoscopic channels that are apparent in SEM image. The digital photograph presents a yellow-colored sample area without surface etching (inset of Fig. 1C).

The electrochemical behaviour of as-formed NiO/TiO_2 layers is investigated using cyclic voltammetry (CV). The measurements were performed in 0.1 M NaOH solution. Specially, because the anodization leads directly to a back-contacted oxide electrode, the NiO/TiO_2 layers grown on the metallic NiTi alloy sheet can be used as an electrode directly without needing a conductive adhesive medium or binders to prepare a functional porous oxide electrode. As shown in Fig. 2A, for the NiO/TiO_2 layers prepared at RT (curve a) and 10°C (curve b), cycling in 0.1 M NaOH solution did not exhibit any clear redox peaks. In contrast, for the sample grown at 0°C (curve c), a pair of well-defined cathodic peak (0.37 V) and anodic peak (0.47 V), corresponding to the Ni(II)/Ni(III) couple, can be clearly in a NaOH solution. However, a main drawback in terms of application is that the nanoscopic channels are too narrow, which limits the diffusion of the electrolyte. Recently, Schmuki *et al.* found for a tight titanium dioxide, if this structure is adequately chemically etched in H_2O_2, a very regular sponge structure can be achieved[29]. When the as-formed NiO/TiO_2 nanostructure (anodized at 0°C) was etched in 30 wt% H_2O_2 under ultrasonication, it is noticed that the peak currents (Fig. 2B) increase with time in the first 20 min, and then the currents become stable. As shown in Fig. 3A, a much more porous structure is observed after H_2O_2 etching treatment if compared with the "as-formed" sample (Fig. 1C). The drastic difference in structure is apparent, which exhibit that the morphology of NiO/TiO_2 layers change to a highly regular and defined nanoporous structure after the H_2O_2 etching treatment. The pore diameter is ranging around 6–10 nm (Fig. 3B). This regular nanoporous structure can be observed over the entire sample surface, and therefore is resulting in a highly enhanced surface area. As shown in Fig. 3C, the thickness of the nanoporous layers is measured as ~ 53 nm. The electrochemical

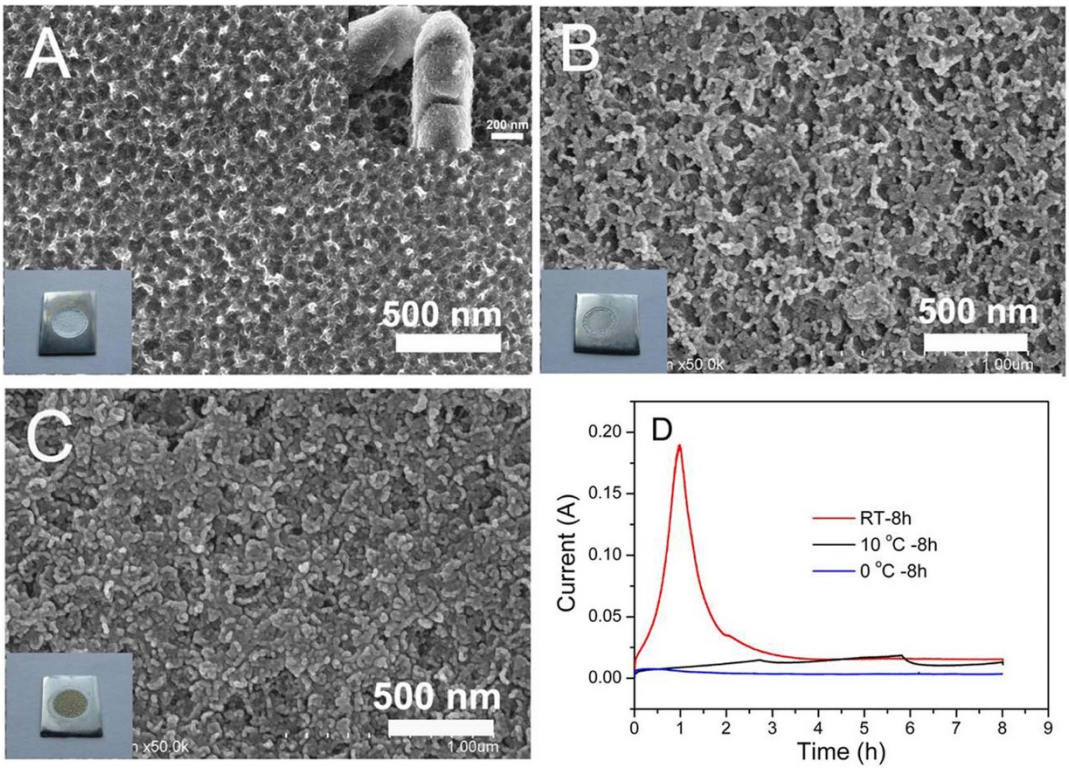

Figure 1 | The SEM and photograph of NiO/TiO_2 nanostructure prepared at (A) room temperature (inset: the peeled off layers), (B) 10°C and (C) 0°C. inset: The digital photograph of the as-formed sample. (D) Anodizing current-time behavior for NiTi alloy at room temperature, 10°C, and 0°C.

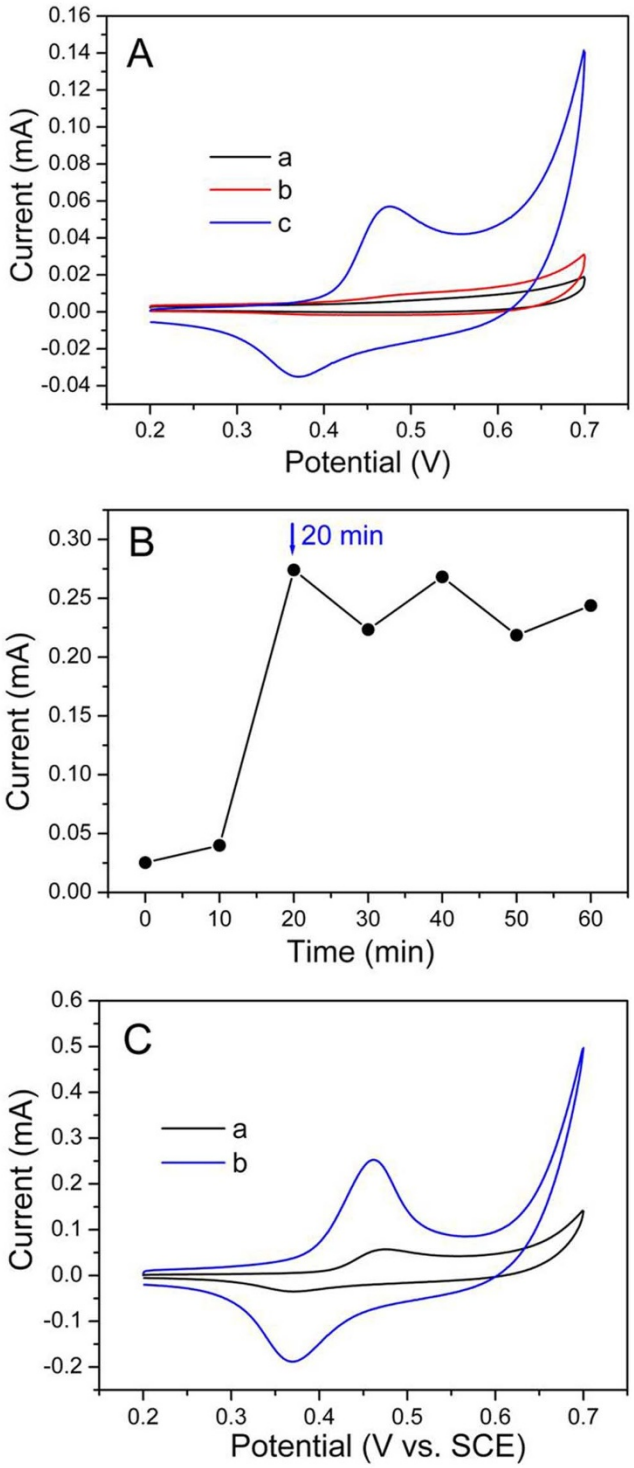

Figure 2 | (A) Cyclic voltammograms of as-formed NiO/TiO_2 nanostructures in 0.1 M NaOH, the samples were anodized at room temperature (curve a), 10°C (curve b) and 0°C (curve c). (B) The influence of ultrasonicated time in H_2O_2 on the anodic peak currents of NiO/TiO_2 layers. (C) Cyclic voltammograms of NiO/TiO_2 layers in 0.1 M NaOH before (curve a) and after (curve b) ultrasonicated for 20 min in 30% H_2O_2. Scan rate: 50 mV s^{-1}.

behaviors of NiO/TiO_2 layers before and after H_2O_2 etching was recorded in Fig. 2C. The advantage of the larger surface area can be seen from the comparison redox peak currents corresponding to the switch of Ni(II)/Ni(III). Obviously, after the etching treatment for 20 min, the electrochemical current of nanoporous NiO/TiO_2 layers (curve b) exhibits a significant enhancement compared to the "as-formed" NiO/TiO_2 nanostructure (curve a). The increase in electrochemical current can be attributed to the morphology change of the sample. To gain information on the composition, energy-dispersive X-ray spectroscopy (EDX) of the H_2O_2 etched samples were acquired. The presence of Ni, Ti and O is revealed by EDX pattern as shown in Fig. 3D. It is evident that the resulted nanoporous layer mainly consists of NiO and TiO_2. The atomic percentages of these three elements were close to the theoretical values, which confirm the formation of nanoporous NiO/TiO_2 hybrid structure.

The effect of potential scan rate (υ) on oxidation peak current and reduction peak current has been investigated in the range of 20−300 mV s^{-1} in Fig. 4A. The anodic and cathodic currents are found to be proportional to the square root of scan rates (inset of Fig. 4A), indicating that electrode reaction is indeed diffusion-controlled since the observed redox peaks involve OH^- diffusion from the support electrolyte to the electrode surface (during the reduction step) or from the electrode surface to the electrolyte (during the oxidation step)[30]. These findings are consistent with the previous reports on NiO nanoparticles and thin layer of $Ni(OH)_2$[31,32]. Stability for nanoporous NiO/TiO_2 layers based electrode was also examined by recording consecutive CV curves in 0.1 M NaOH solution, and the results are plotted in Fig. 4B. After scanning for 30 cycles, no obvious decrements in the anodic and cathodic peak current can be detected, which indicating that the resulted nanoporous NiO/TiO_2 structure has very excellent electrochemical stability in the basic media, and thus can be applied as the electrode materials to construct biosenors.

To demonstrate the functional potential of these ordered nanoporous NiO/TiO_2 structure in the construction of biosensors, electrochemical oxidation of glucose were carried out. The measurements were performed in 0.1 M NaOH solution with the addition of a certain amount of glucose. Fig. 5A present the CVs of NiO/TiO_2 electrode in the absence (curve a) and presence (curve b) of 1 mM glucose in 0.1 M NaOH. Upon the addition of glucose, due to the catalytic effect of the redox Ni(II)/Ni(III) couple for oxidation of glucose to gluconolactone, Ni(III) can be deoxidized to Ni(II). Therefore, the presence of glucose could leads to an increase in anodic peak current. As a comparison, anodized TiO_2 layer exhibits negligible response (~300 fold lower than that of nanoporous NiO/TiO_2 layers) with the addition of glucose (Fig. 5B). These results indicate that TiO_2 is not an active electrode material to catalyze glucose eletroxidation and the observed electrocatalytical activities originate from NiO in the nanoporous film.

Fig. 5C exhibits the amperometric response of the NiO/TiO_2 nanoporous electrodes at 0.52 V upon successive addition of glucose. The electrode exhibit a sensitive response even for 5 μM glucose (inset of Fig. 5C), which can be attributed to the good electrocatalytic activity and 3D nanoporous structure of NiO/TiO_2 film. As plotted in Fig. 5D, the calibration plot is linear over a broad concentration range of 0.005−12.1 mM with a correlation coefficient of 0.999, a sensitivity of 252.0 μA mM^{-1} cm^{-2}. The current deviates from linearity at higher glucose concentration. As it is known to occur in alkaline media, this deviation can be due to the passivation of the electrode and/or the formation of glucose isomer[33]. Considering the detection limit as 3 time of the noise level, the detection limit for the proposed electrode was obtained as 1.0 μM. In a practical use of nonenzymatic glucose sensors, specificity is another important point that needs attention. Typically, interference (competing red/ox pairs) occurs under physiological conditions originating from ascorbic acid (AA), uric acid (UA), and p-acetamidophenol (AP); the normal physiological level of glucose is 3–8 mM, while the concentration of endogenous AA and UA is about 0.125 mM and 0.33 mM in bood sample, respectively[34]. The NiO/TiO_2 nanoporous electrode shows

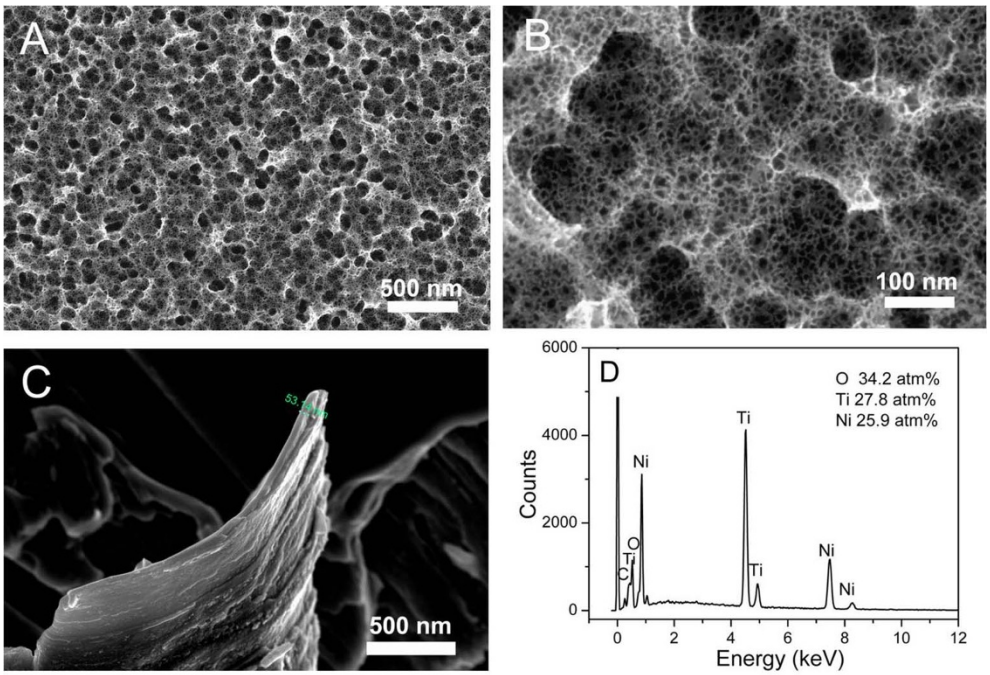

Figure 3 | Top (A, B) and side (C) views of SEM images of the nanoporous anodic layer after sonicated for 20 min in 30% H_2O_2. (D) EDX spectra of the resulted nanoporous NiO/TiO_2 layers.

a satisfied anti-interference ability in the alkaline medium. For example, addition of 100 μM uric acid, ascorbic acid and p-acetamidophenol has no obvious influence on the current responses toward 4 mM glucose in 0.1 M NaOH. Moreover, when the proposed NiO/TiO_2 nanoporous electrode is dried first and then kept in a dry condition at room temperature, the catalytic current for glucose didn't show any obvious decrese after a storage period of 30 days, thus exhibiting long-term stability.

Discussion

In the current work, we prepared nanoporous NiO/TiO_2 layers by a combination of electrochemical anodization and subsequent selective etching. It's a very simple and efficient approach to prepare sensing platforms. The as-prepared nanoporous structure is mechanically and chemically stable. And this regular nanoporous structure can be observed over the entire sample surface, which leads to a highly enhanced surface area. Another major advantage is that the fabrication of the presented nanoporous NiO/TiO_2 layers based electrode does not need polymer binders that are commonly used in conventional non-enzymatic glucose sensor. The polymer binders typically are not electrochemically active for glucose sensing, and could potentially block the catalytic sites on the NiO surface.

Upon addition of glucose, a significant enhancement in anodic peak current can be observed - this is attributed to the electrooxidation of glucose to glucolactone by Ni(III). As indicated in literatures, the oxidation of glucose on the surface NiO in basic media is catalyzed by NiO/NiOOH redox couple as follows[11,35]:

$$NiO + OH^- \rightarrow NiO(OH) + e^- \quad (1)$$

$$NiO(OH) + \text{glucose} \rightarrow NiO + OH^- + \text{glucolactone} \quad (2)$$

Once Ni(III) species is formed on the electrode, it rapidly oxidizes glucose during the anodic scan, sacrificing Ni(III) and producing Ni(II) species, which in turn is oxidized again under the anodic voltage. That means on the reverse scan glucose still is oxidized by available surface Ni(III), i.e., the cathodic peak is smaller than in the glucose free case. As a result, the change in the concentration of Ni(II) and Ni(III) species cause the increase of the anodic peak

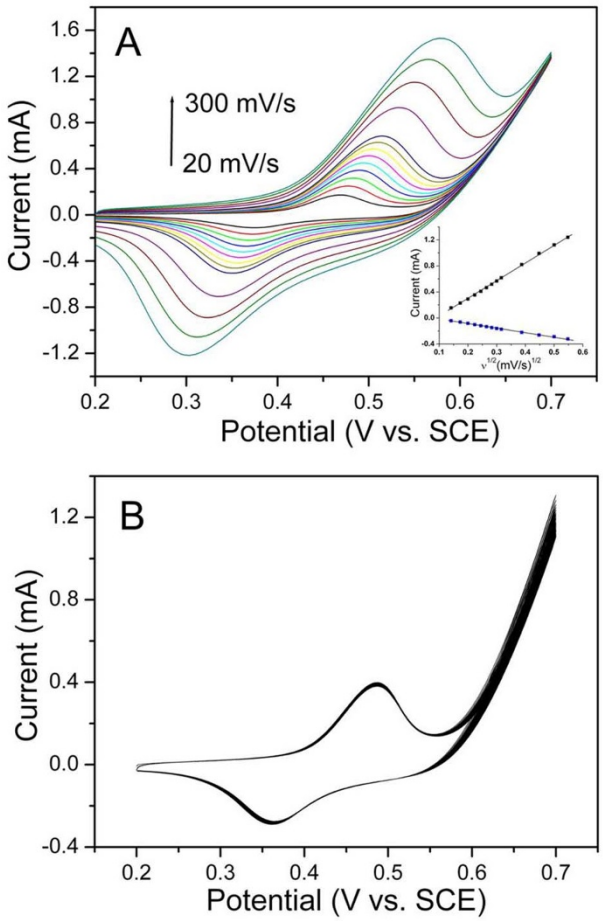

Figure 4 | (A) Cyclic voltammograms of the nanoporous NiO/TiO_2 layer based electrode at various scan rates in 0.1 M NaOH. Inset: plots of the anodicand cathodic peak currents vs. the square root of the potential scan rate. (B) The stability test showing cyclic voltammograms for the 30 cycles at a scan rate of 50 mV s^{-1}.

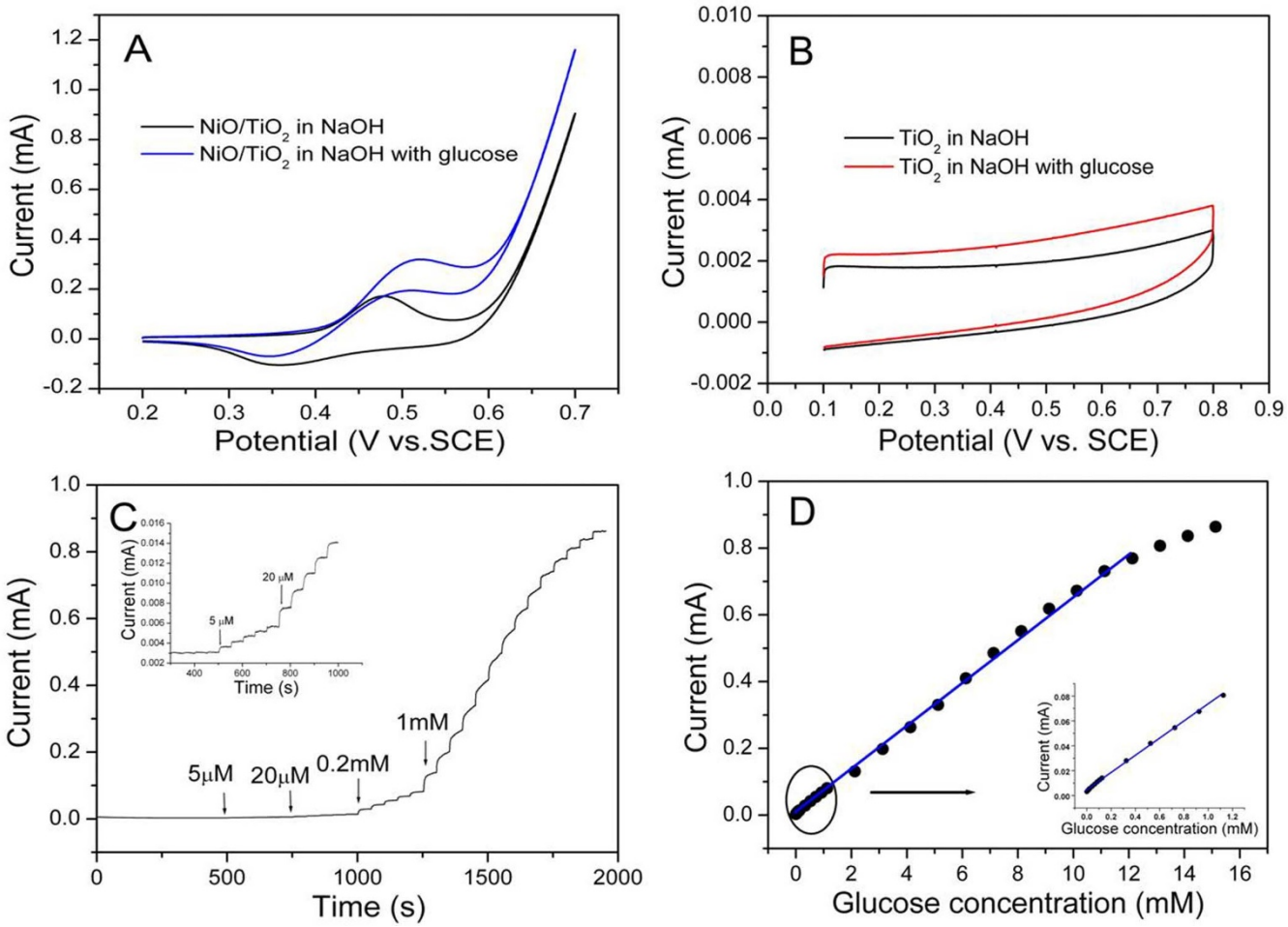

Figure 5 | Cyclic voltammograms of the nanoporous (A) NiO/TiO_2 and (B) TiO_2 layers based electrode in 0.1 M NaOH in the absence and presence of 1 mM glucose at a scan rate of 50 mV s^{-1}. (C) Amperometric response at the NiO/TiO_2 electrode for successive addition of different concentrations of glucose. (D) Corresponding linear calibration curve of glucose concentration.

current and the decrease of the cathodic peak current, as observed from Fig. 5A.

The detection limit, linear range and sensitivity of the resulted NiO/TiO_2 electrode were compared with several typical metal and metal oxide electrode for glucose non-enzymatic detection, which are summarized in Table 1. Clearly, the present nanoporous NiO/TiO_2 structure based electrode exhibits lower detection limit, wide linear range and satisfied sensitivity compared to those earlier reports. The 3D-ordered NiO/TiO_2 layers based electrode could be easily prepared by electrochemical anodization technique. And this regular nanoporous structure can be observed over the entire sample surface. The improved sensitivity and linear range can be assigned to the nanoporous structure with large effective surface area, interconnected microenvironments, improved mechanical and chemical stablility.

In summary, we report for the first time the formation of nanoporous NiO/TiO_2 layers by using self-organizing electrochemical anodization. By optimized the temperature during anodization, the dissolution of NiO/TiO_2 layers can be sufficiently suppressed. In the present case a high-ordered nanoporous structure is formed upon chemical etching in a H_2O_2 solution under ultrasonication. We demonstrate that the resulted nanoporous NiO/TiO_2 layers have a

Table 1 | Sensing characteristics of the different non-enzymatic glucose sensors

Electrode	Sensitivity ($\mu AmM^{-1}cm^{-2}$)	Liner range (mM)	Detection limit (μM)	Stability	Reference
NiO nanoflake arrays	8500	0.01–0.80	1.2	–	[11]
NiO/C-Ti	582.6	0.002–2.6	2	60 days	[36]
$Ni(OH)_2/TiO_xC_y$	240	0.02–11.0	5.0	30 days	[37]
$NiO\text{-}TiO_2NTA$[a]	200.0	0.1–1.7	4.0	–	[38]
NiO/CPE[b]	55.9	0.001–0.11	0.16	28 days	[30]
NiO-CdO/GCE[c]	212.7	0.02–6.4	0.35	–	[39]
NiO/MWCNTs[d]	–	0.2–12	160	70 days	[40]
NiO/TiO_2	252.0	0.005–12.1	1.0	>30 days	Present work

[a]TiO_2 nanotube arrays.
[b]Fluorine-doped tin oxide glass.
[c]Glassy carbon electrode.
[d]Multiwalled carbon nanotubes.

significant potential for application such as the electrode materials with high sensitivity and wide detection range for glucose sensing.

Methods

Materials. NiTi foil (1 mm thickness, with 50.6 at.% Ni contents) was obtained from Baosheng Metal Co. (Baoji, China). Ammonium fluoride (NH_4F) and glucose were purchased from Sigma-Aldrich Chemicals Co. Sodium hydroxide (NaOH), ethylene glycol, glycerol, acetone, isopropanol, and methanol and other chemicals were of analytical grade and used without further purification. All aqueous solutions were prepared with deionized water (>18 MΩ).

Preparation of nanoporous NiO/TiO_2 layers. Rectangular samples of 15 mm × 15 mm × 1 mm were cut from a NiTi (50.6 at% Ni) sheet and the sharp corners rounded by grinding with SiC paper. The surface of the samples was ground and polished to a mirror finish before use. Prior to the anodization process, the foils were cleaned by sonicating in acetone, isopropanol, and methanol, followed by rinsing with deionized (DI) water and drying the samples in a N_2 stream. Anodization was carried out using a voltage potentiostat in a two-electrode system with the sample being the working electrode and a platinum gauze serving as counter electrode. All electrolytes were cooled in a refrigerator before use. During anodization, the substrate temperature was controlled via a water cooling plate which connected to the back contact copper plate to effectively control the temperature of the NiTi foil and pumped out the heat by using a thermostat. Anodization was carried out at different temperatures of electrolyte (RT, 0°C and 10°C) for various times to grow nanoporous layers. For the best condition anodization, the substrates were polarized at 40 V in mixed ethylene glycol and glycerol solvent with a volume ratio of 1 to 3, containing 3 M H_2O and 0.54 M NH_4F. After anodization, the nanotube layers were sonicated in ethanol for 15 min, and dried in a nitrogen stream. For selective etching treatments, the anodized samples were sonicated in 30 wt% H_2O_2. After treatment, the samples were rinsed with DI and dried in a nitrogen stream.

Instruments. The morphologies of the anodized layers before and after particle decoration were characterized using a field-emission scanning electron microscope (Hitachi FE-SEM S4800). The cyclic voltammograms and chronoamperometric measurements were performed using a CHI660D electrochemical workstation (CH Instrument Co. Shanghai). For electrochemical measurements, a conventional three electrode system was used. The nanoporous NiO/TiO_2 layers acted as the working electrodes (8 mm in electrode diameter). A Pt foil and a saturated calomel electrode (SCE) were used as the counter and reference electrodes, respectively. In all electrochemical investigations, a degassed 0.1 M NaOH solution was employed as the supporting electrolyte.

1. Updike, S. J. & Hicks, G. P. The enzyme electrode. *Nature* **214**, 986–988 (1967).
2. Wang, J. Electrochemical glucose biosensors. *Chem. Rev.* **108**, 814–825 (2008).
3. Clark, L. C. & Lyons, C. Electrode systems for continuous monitoring in cardiovascular surgery. *Ann. NY Acad. Sci.* **102**, 29–45 (1962).
4. Song, Y. Y., Zhang, D., Gao, W. & Xia, X. H. Nonenzymatic glucose detection by using a three-dimensionally ordered, macroporous platinum template. *Chem. Eur. J.* **11**, 2177–2182 (2005).
5. Yuan, J. H., Wang, K. & Xia, X. H. Highly ordered platinum-nanotubule arrays for amperometric glucose sensing. *Adv. Funct. Mater.* **15**, 803–809 (2005).
6. Zhou, Y. G., Yang, S., Qian, Q. Y. & Xia, X. H. Gold nanoparticles integrated in a nanotube array for electrochemical detection of glucose. *Electrochem. Commun.* **11**, 216–219 (2009).
7. Rong, L. Q., Yang, C., Qian, Q. Y. & Xia, X. H. Study of the nonenzymatic glucose sensor based on highly dispersed Pt nanoparticles supported on carbon nanotubes. *Talanta* **72**, 819–824 (2007).
8. Li, Y., Song, Y. Y., Yang, C. & Xia, X. H. Hydrogen bubble dynamic template synthesis of porous gold for nonenzymatic electrochemical detection of glucose. *Electrochem. Commun.* **9**, 981–988 (2007).
9. Park, S., Chung, T. D. & Kim, H. C. Nonenzymatic glucose detection using mesoporous platinum. *Anal. Chem.* **75**, 3046–3049 (2003).
10. Bai, H. Y., Han, M., Du, Y. Z., Bao, J. C. & Dai, Z. H. Facile synthesis of porous tubular palladium nanostructures and their application in a nonenzymatic glucose sensor. *Chem. Commun.* **46**, 1739–1741 (2010).
11. Wang, G. *et al.* Free-standing nickel oxide nanoflake arrays: synthesis and application for highly sensitive non-enzymatic glucose sensors. *Nanoscale* **4**, 3123–3127 (2012).
12. Li, X. *et al.* Preparation of nickel oxide and carbon nanosheet array and its application in glucose sensing. *J. Solid State Chem.* **184**, 2738–2743 (2011).
13. Cheng, W. L., Sue, J. W., Chen, W. C., Chang, J. L. & Zen, J. M. Activated nickel platform for electrochemical sensing of phosphate. *Anal. Chem.* **82**, 1157–1161 (2010).
14. Fleischmann, M., Korinek, K. & Pletcher, D. The kinetics and mechanism of the oxidation of amines and alcohols at oxide-covered nickel, silver, copper, and cobalt electrodes. *J. Chem. Soc. Perkin. Trans.* **2**, 1396–1403 (1972).
15. Ali, M. A. *et al.* Highly efficient bienzyme functionalized nanocomposite-based microfluidics biosensor platform for biomedical application. *Sci. Rep.* **3**, 2661 (2013).
16. Su, D. W., Ford, M. & Wang, G. X. Mesoporous NiO crystals with dominantly exposed {110} reactive facets for ultrafast lithium storage. *Sci. Rep.* **2**, 924 (2012).
17. Marioli, J. M., Luo, P. F. & Kuwana, T. Nickel-chromium alloy electrode as a carbohydrate detector for liquid chromatography. *Anal. Chim. Acta* **282**, 571–580 (1993).
18. Luo, P. F. & Kuwana, T. Nickel-titanium alloy electrode as a sensitive and stable LCEC detector for carbohydrates. *Anal. Chem.* **66**, 2775–2782 (1994).
19. Masuda, H. & Fukuda, K. Ordered metal nanohole arrays made by a two-step replication of honeycomb structures of anodic alumina. *Science* **268**, 1466–1468 (1995).
20. Zwilling, V. *et al.* Structure and physicochemistry of anodic oxide films on titanium and TA6V alloy. *Surf. Interface Anal.* **27**, 629–637 (1999).
21. Lee, K. *et al.* Anodic formation of thick anatase TiO_2 mesosponge layers for high-efficiency photocatalysis. *J. Am. Chem. Soc.* **132**, 1478–1479 (2010).
22. Roy, P., Berger, S. & Schmuki, P. TiO_2 nanotubes: Synthesis and applications. *Angew. Chem. Int. Ed.* **50**, 2904–2939 (2011).
23. Yang, Y., Albu, S. P., Kim, D. & Schmuki, P. Enabling the anodic growth of highly ordered V_2O_5 nanoporous/nanotubular structures. *Angew. Chem. Int. Ed.* **50**, 9071–9075 (2011).
24. Albu, S. P., Ghicov, A. & Schmuki, P. High aspect ratio, self-ordered iron oxide nanopores formed by anodization of Fe in ethylene glycol/NH_4F electrolytes. *Phys. Status Solidi RRL* **3**, 64–66 (2009).
25. Mohapatra, S. K., John, S. E., Banerjee, S. & Misra, M. Water photooxidation by smooth and ultrathin Alpha-Fe_2O_3 nanotube arrays. *Chem. Mater.* **21**, 3048–3055 (2009).
26. LaTempa, T. J., Feng, X., Paulose, M. & Grimes, C. A. Temperature-dependent growth of self-assembled hematite (Alpha-Fe_2O_3) nanotube arrays: Rapid electrochemical synthesis and photoelectrochemical properties. *J. Phys. Chem. C* **113**, 16293–16298 (2009).
27. Lee, C. Y., Lee, K. & Schmuki, P. Anodic formation of self-organized cobalt oxide nanoporous layers. *Angew. Chem. Int. Ed.* **52**, 2077–2081 (2013).
28. Yang, M., Yang, G., Spiecker, E., Lee, K. & Schmuki, P. Ordered "superlattice" TiO_2/Nb_2O_5 nanotube arrays with improved ion insertion stability. *Chem. Commun.* **49**, 460–462 (2013).
29. Kim, D. *et al.* Formation of a mom-thickness-limited titanium dioxide mesosponge and its use in dye-sensitized solar cells. *Angew. Chem. Int. Ed.* **48**, 9326–9329 (2009).
30. Mu, Y., Jia, D., He, Y., Miao, Y. & Wu, H.-L. Nano nickel oxide modified non-enzymatic glucose sensor with enhanced sensitivity through an electrochemical process strategy at high potential. *Biosens. Bioelectro.* **26**, 2948–2952 (2011).
31. Salimi, A. & Roushani, M. Non-enzymatic glucose detection free of ascorbic acid interference using nickel powder and nafion sol–gel dispersed renewable carbon ceramic electrode. *Electrochem. Commun.* **7**, 879–887 (2005).
32. You, T. *et al.* An amperometric detector formed of highly dispersed Ni nanoparticles embedded in a graphite-like carbon film electrode for sugar determination. *Anal. Chem.* **75**, 5191–5196 (2003).
33. Oncescu, V. & Erickson, D. High volumetric power density, non-enzymatic, glucose fuel cells. *Sci. Rep.* **3**, 1226 (2013).
34. Ding, Y. *et al.* Electrospun Co3O4 nanofibers for sensitive and selective glucose detection. *Biosens. Bioelectron.* **26**, 542–548 (2010).
35. Zheng, H., Xue, H. G., Zhang, Y. F. & Shen, Z. Q. A glucose biosensor based on microporous polyacrylonitrile synthesized by single rare-earth catalyst. *Biosens. Bioelectron.* **17**, 541–545 (2002).
36. Li, X. *et al.* Preparation of nickel oxide and carbon nanosheet array and its application in glucose sensing. *J. Solid State Chem.* **184**, 2738–2743 (2011).
37. Gao, Z. D. *et al.* Nickel Hydroxide Nanoparticle Activated Semimetallic TiO_2 Nanotube Arrays for Nonenzymatic Glucose Sensing. *Chem. Eur. J.* **19**, 15530–15534 (2013).
38. Wang, C., Yin, L., Zhang, L. & Gao, R. Ti/TiO_2 nanotube array/Ni composite electrodes for nonenzymatic amperometric glucose sensing. *J. Phys. Chem. C* **114**, 4408–4413 (2011).
39. Ding, Y., Wang, Y., Zhang, L., Zhang, H. & Lei, Y. Preparation, characterization and application of novel conductive NiO-CdO nanofibers with dislocation feature. *J. Mater. Chem.* **22**, 980–986 (2012).
40. Shamsipur, M., Najafi, M. & Milani Hosseini, M. R. Highly improved electrooxidation of glucose at a nickel(II) oxide/multi-walled carbon nanotube modified glassy carbon electrode. *Bioelectrochem.* **77**, 120–124 (2010).

Acknowledgments

The National Natural Science Foundation of China (21005012, 21275026, 11174046, 21322504), the program for New Century Excellent Talents in University of China (NCET-10-0305), and the Fundamental Research Funds for the Central Universities (N120505002, N120505006, N110805001, N110705002) is gratefully acknowledged.

Author contributions

Z.-D.G. and Y.-Y.S. conducted the research and discussed the results. Y.H. and Y.W. prepared the anodized samples. Y.H. carried out the electrochemical experiments. Z.-D.G., J.X. and Y.W. carried out the materials characterizations. Z.-D.G. drafted the paper and the

Supplementary Information. All of the authors reviewed the manuscript and participated in discussions on the results of this research.

Additional information

Competing financial interests: The authors declare no competing financial interests.

How to cite this article: Gao, Z.-D., Han, Y.Y., Wang, Y.M., Xu, J.W. & Song, Y.-Y. One-Step to Prepare Self-Organized Nanoporous NiO/TiO_2 Layers and its Use in Non-Enzymatic Glucose Sensing. *Sci. Rep.* **3**, 3323; DOI:10.1038/srep03323 (2013).